Assessment of Liquid Metals as Heat Transfer Fluid for Parabolic Trough Solar Collector

Krishna Chaitanya Nvv[1], Ravi Kumar K[2]

[1] Student, University of Petroleum and Energy Studies, Dehradun (India)

[2] Assistant Professor, Centre for Energy Studies, Indian Institute of Technology Delhi, New Delhi (India)

Abstract

In this article, heat transfer characteristics of various heat transfer fluids (HTF's) such as water, therminol oil, molten salt and liquid metals are studied for parabolic trough solar collector. A three dimensional (3-D) numerical simulation of absorber for parabolic trough solar collector is carried out using commercial computational fluid dynamics software Fluent 16.0. The numerical model is solved based on K- ε turbulent model with standard wall function. The influence of thermo-physical properties of HTF's on heat transfer rate from the absorber wall surface to the fluid is studied for various mass flow rates ranging from 0.5 kg/s to 1.5 kg/s insteps of 0.25 kg/s. The analysis is carried out for both uniform and non-uniform heat flux at the absorber wall surface. For both uniform and non-uniform heat flux configuration, liquid sodium offers better heat transfer characteristics among all the heat transfer fluids. Among all the heat transfer fluids, liquid sodium offers less temperature gradient (8.58 K) and therminol oil offers high temperature gradient (42.74 K) around the circumference of the absorber for the mass flow rate of 1 kg/s. Hence, liquid sodium offers significant benefits in terms of performance enhancement compared to other heat transfer fluids.

Key Words: Parabolic trough solar collector, Receiver, Variable heat flux, Heat transfer fluid, Liquid sodium

1. Introduction

A concentrated solar thermal collector concentrates solar radiation on the receiver that converts solar radiation in to useful high temperature heat. There are four concentrated solar thermal power (CSTP) technologies namely linear Fresnel reflector (LFR), parabolic trough collector (PTC), power tower (PT) and parabolic dish collector (PDC) that have reached reasonably high state of maturity. Globally ~ 4.8 GW CSTP plants are in operation and ~1.6 GW capacity of power plants are under construction as on March 2017 (NREL, 2017). Among the CSTP technologies, PTC is most proven technology and commercially available for power generation with potential of high dispatchability. The parabolic trough collector consists of parabolic shaped concentrator, receiver and supporting structure. Receiver is the most important component of the CSTP system. The PTC receiver consists of an absorber tube surrounded by glass envelope with annulus space evacuated. Heat transfer fluid is circulated through the receiver to collect the heat from the receiver. Typically organic or synthetic oils are used as a heat transfer fluid (HTF) in the PTC system. Synthetic oil has poor heat transfer characteristics and it has limitation of maximum operating temperature (< 400^{o}C). Design of receiver and heat losses from the receiver plays an important role on the performance of PTC. Heat losses from the receiver is the function of absorber temperature, ambient temperature, absorber type, wind velocity, etc. The temperature of the absorber may be reduced by increasing the heat transfer rate between inner wall surface of the absorber to the fluid.

There are few studies exist on enhancement of heat transfer rate from the absorber wall surface to the fluid. Almanza et al., (1997) conducted the experiments to study the deflection of absorber tubes due to temperature gradient in circumferential direction for direct steam generation in parabolic collector. Odeh et al., (1998) studied the performance of parabolic trough solar collector with synthetic oil and water as HTF. Kumar and Reddy (2009, 2012) studied the porous disc receiver for parabolic trough collector with therminol-55 and water as HTF and developed the empirical correlations for Nusselt number and friction factor. Cheng et al., (2010) performed the coupled flux distribution and heat transfer model for parabolic trough solar collector to analyze the heat distribution in the receiver. In recent days, liquid metals gaining much attention for CSTP applications as HTF. Boerema et al. (2012) studied liquid sodium and Hitec (a ternary molten salt 53% KNO_3 + 40% $NaNO_2$ + 7%

doi:10.18086/swc.2017.04.06 Available at http://proceedings.ises.org

$NaNO_3$) as heat transfer fluids and reported that both fluids are alternative for molten salts in PT systems for power generation. Kotze et al. (2012) compares the strengths and limitations of various HTF's for CSTP applications and proposed NaK may be the primary HTF for performance improvement. Pacioa et al. (2013) proposed liquid metals such as liquid sodium and lead-bismuth eutectic as efficient heat transfer fluids for PT systems. The recent development in HTF's for low, medium and high temperature solar thermal systems has been reviewed by Srivastva et al. (2015). Overall, liquid metals gaining momentum for CSTP applications to improve the performance of the receiver. In this paper, heat transfer ability of various HTF's and temperature gradient around the circumference of the absorber tubes are explored. The characteristics of HTF's such as stability at higher temperature, decomposition due to continuous heating and cooling, corrosion issues will be studied in future as continuation of this work.

2. Modeling of Absorber for Parabolic Trough Solar Collector

A 3-D numerical modeling is carried out to investigate the heat transfer rate from the absorber wall inner surface to the various working fluids such as water, therminol oil, molten salt, liquid sodium and eutectic NaK (77.8 % potassium and 22.2 % sodium by weight). The eutectic NaK hereafter referred as NaK78. The thermo-physical properties of various heat transfer fluids are given in Table 1. The schematic of absorber of parabolic trough solar collector is shown in Figure 1. The absorber of 4 m length is considered for the analysis with internal and external diameter of 66 mm and 70 mm respectively. The mass flow inlet and pressure outlet boundary condition is considered. The analysis is carried out for various mass flow rate ranging from 0.5 kg/s to 1.5 kg/s insteps on 0.25 kg/s. Constant and variable heat flux boundary conditions are considered for the analysis. For constant heat flux boundary condition, the absorber wall is subjected to 21000W/m^2 and for variable heat flux boundary conditions, the flux profile is given in Figure 2 (Khanna and Sharma, 2016).

Tab. 1: Thermo-physical properties of various heat transfer fluids (Kotze, 2012)

S. No.	Heat Transfer Fluid	Density (kg/m^3)	Specific Heat (kJ/kg K)	Thermal Conductivity (W/m K)
1	Water	995.7	4.178	0.60
2	Therminol Oil	1056	2.5	0.09
3	Molten salt	1794	1.21	0.55
4	Liquid Sodium	820	1.25	119.3
5	NaK78	749	0.94	26.2

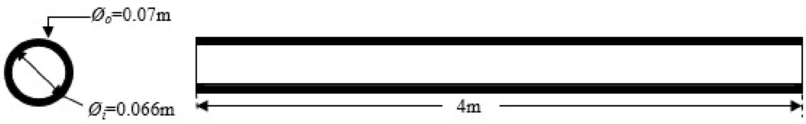

Fig. 1 Schematic of absorber of a parabolic trough solar collector

The governing equations for steady, incompressible, forced convection in the absorber are given as (FLUENT, 2016):

Continuity equation:

$$\nabla \vec{V} = 0 \quad \text{(eq. 1)}$$

Momentum equation:

$$\vec{V}\nabla\left(\vec{V}\right) = -\frac{\nabla P}{\rho} + \left(\frac{\mu + \mu_t}{\rho}\right)\nabla^2\left(\vec{V} + \vec{V}^T\right) + \overrightarrow{F_B} \quad \text{(eq. 2)}$$

Energy equation:

$$\rho C_p \nabla\left(\vec{V}T\right) = \lambda \nabla^2 T \quad \text{(eq.3)}$$

A steady state, 3-D model with incompressible and turbulent flow is solved using K- ε turbulent model. Reynolds Averaged Navier Stokes (RANS) model is used to solve the momentum equation with turbulent stresses. The RANS equations for incompressible flow is:

$$\frac{\partial}{\partial x_j}\overline{(u_i u_j)} = -\frac{1}{\rho_f}\frac{\partial \overline{p}}{\partial x_j} + \frac{\partial}{\partial x_j}\left[\vartheta_{eddy}\left(\frac{\partial u_i}{\partial x_j} + \frac{\partial u_j}{\partial x_i}\right)\right] \quad \text{(eq. 3)}$$

where, $\vartheta_{eddy} = C_\mu \frac{k^2}{\varepsilon}, C_\mu = 0.0845, k = 0.71\varepsilon^{2/3}L^{2/3}$

k and ε are the values of turbulent kinetic energy and turbulent dissipation rate.

The heat transfer coefficient from the absorber tube to the fluid may be given as:

$$h_f = \frac{q^"}{T_w - T_{ref}} \quad \text{(eq. 4)}$$

Where, $q^"$ is heat flux, T_w is the wall temperature and T_{ref} is reference temperature.

3. Boundary Conditions for Receiver

The following boundary conditions are applied for modeling of the absorber of the parabolic trough solar collector:

a) Inlet boundary condition

Mass flow inlet boundary condition is used at the absorber inlet with different temperature depends on the working fluid.

$$u = u_{in}; T_f = T_{in} \; at \; L = 0$$

$$0 \le r \le \frac{d_i}{2}, \; -180^o \le \theta \le 180^o \quad \text{(eq. 5)}$$

Since the melting temperature of molten salt and liquid metals are higher than the ambient temperature, the inlet temperature for various HTF's are considered as 300 K for water, therminol oil and NaK 78, 371 K for liquid sodium and 498 K for molten salt.

b) Wall boundary condition
Absorber inner wall:

No slip boundary condition is given to the inner and outer side of the wall.

$$u = 0 \; at \; 0 \le L \le 4, \; r = \frac{d_i}{2}, \; -180^o \le \theta \le 180^o \quad \text{(eq. 6)}$$

Absorber outer wall is subjected to heat flux boundary condition. Two boundary conditions are applied to study the performance of the absorber (a) Uniform (constant) heat flux boundary condition: the absorber wall is subjected to uniform heat flux of 21000W/m^2 and (b) Non-Uniform heat flux boundary conditions: the heat flux profile applied on the absorber wall surface is given in Figure 2 (Khanna and Sharma, 2016). In figure 2, zero degree corresponds to bottom of the absorber tube and ± 180^o corresponds to top of the absorber.

c) Pressure outlet boundary condition is employed across the outlet of the receiver.

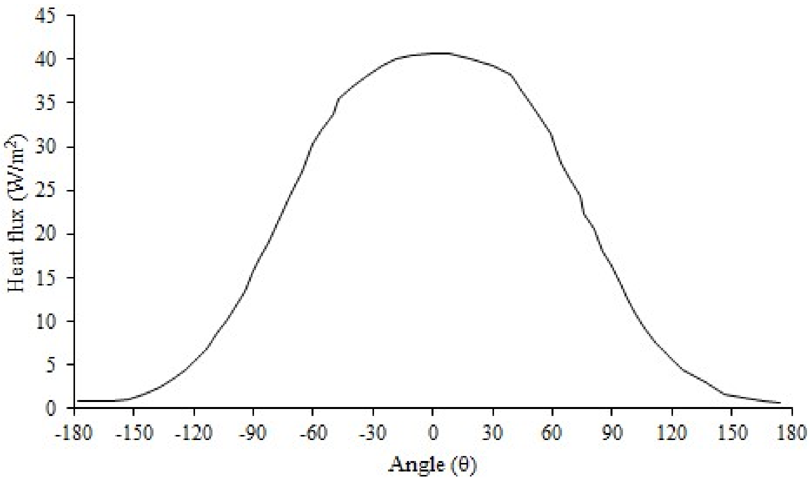

Fig. 2: Heat flux profile applied on the absorber surface (Khanna and Sharma, 2016)

4. Numerical Procedure

The governing equations are solved by finite volume method using CFD commercial software ANSYS Fluent 16.0 with segregated implicit solver and first order formulation (FLUENT, 2016). The first order discretization technique is used in pressure based solver. The velocity and pressure coupling is done by using SIMPLE algorithm. A convergence criteria of 10^{-3} is applied for velocity and momentum equations and 10^{-7} is applied for energy equation. The computational model is created in ANSYS 16.0 geometry module. The model is discretized into quadrilateral elements using ANSYS meshing module. Grid independence study is carried out and the number of mesh element is identified as 688539 cells. The variation of results are insignificant beyond the above mentioned element size. The geometric parameters of the absorber consists of a cylindrical tube with 4 m length having an inner diameter of 0.066 m and an outer diameter of 0.07 m. The computational domain consists of two zones such as solid and fluid. The wall is a solid zone where uniform and non-uniform heat flux is applied in two separate cases as discussed earlier. The fluid zone is the heat transfer fluid flowing the through the cylinder from inlet to outlet.

5. Validation

The model is validated by comparing the Nusselt number of present numerical model with Dittus-Boelter correlation. The result shows that the present model deviates from Dittus-Boelter correlation is around 9%.

The Dittus-Boelter equation is given as:

$$Nu = 0.023 Re^{0.8} Pr^{0.4} \qquad \text{(eq. 7)}$$

for $Re \geq 10,000$ *and* $0.7 \leq Pr \leq 160$

6. Results and Discussion

The numerical simulation of the absorber of a parabolic trough solar collector is carried out to analysis the influence of thermo-physical properties of various HTF's on heat transfer rate from absorber inner wall surface to the fluid with different mass flow rates. The HTF's mass flow rate varies from 0.5 kg/s to 1.5 kg/s insteps of 0.25 kg/s. In first case, simulations are carried out for the constant heat flux boundary condition to compare the heat transfer coefficients and temperature difference (ΔT) between the absorber wall surface and mean fluid temperature. The heat transfer coefficient increases with mass flow rate for all the HTF's. As shown in Figure 3 that the maximum heat transfer coefficient as 1268 W/m^2K at 1.5 kg/s is achieved for liquid sodium. For mass flow rate of 1 kg/s, the minimum ΔT is observed for liquid sodium as 1.38 K and maximum ΔT is observed for therminol oil as 31 K (Figure 4). It shows clearly that thermal conductivity of the HTF plays an important role in heat transfer from absorber wall to the fluid. Also, it helps to reduce the absorber wall temperature that results in reduced heat losses from the absorber.

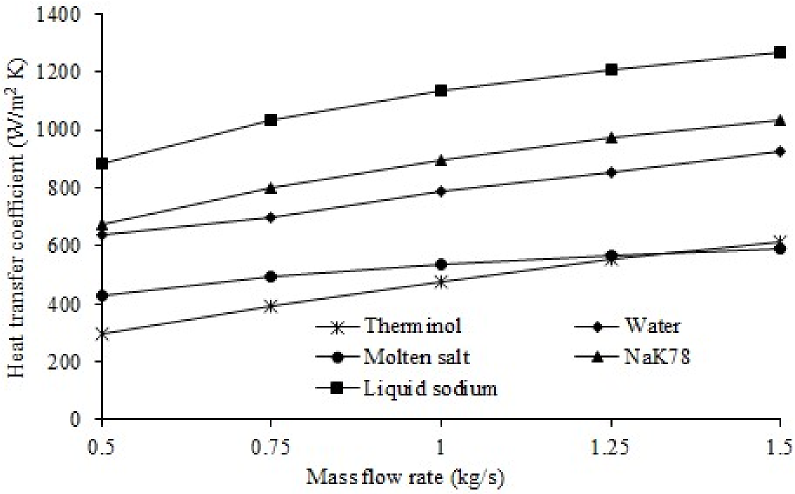

Fig. 3: Heat transfer coefficient for the absorber tube of parabolic trough solar collector for various HTF's with uniform heat flux boundary condition

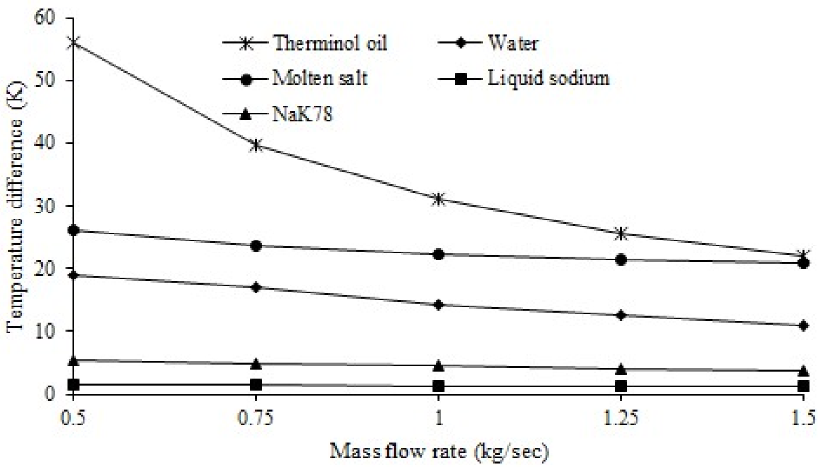

Fig. 4: Temperature difference between the absorber wall surafce and mean fluid temperature for various HTF's with uniform heat flux boundary condition

In second case, non-uniform heat flux boundary condition is applied around the absorber circumference to evaluate the heat transfer coefficient from wall to the fluid, temperature difference between the absorber inner wall surface to the mean fluid temperature and variation of temperature around the absorber circumference. Figure 5 shows that the surface heat transfer coefficient increases with flow rate. For 1.5 kg/s of mass flow rate, the maximum heat transfer coefficient of 1100 W/m^2 K is observed for liquid sodium and minimum of 600 W/m^2 K is observed for therminol oil. It is observed that the temperature difference between the inner wall surface to the mean fluid temperature (ΔT) is gradually decreases with increase in mass flow rate. Among all the HTF's, the maximum and minimum temperature difference occurs for therminol oil and liquid sodium respectively for the given mass flow rate.

Temperature of the absorber around the circumference for 0.5 kg/s and 1.5 kg/s is shown in Figure 7 and 8 respectively. Since the inlet temperature of liquid sodium and molten salt is higher than the other HTF's, the absorber wall temperature also higher for liquid sodium and molten salt. At bottom of the absorber wall is subjected to higher heat flux (figure 2) and it decreases around the circumference while moving to top of the absorber. For most of the HTF's, higher wall temperature is observed at bottom of the absorber tube (0°). Absorber wall temperature around the circumference is almost constant for liquid sodium. The temperature difference around the circumference of the wall in descending is observed as therminol oil followed by molten salt, water, NaK78 and liquid sodium for the given mass flow rate (Table 2).

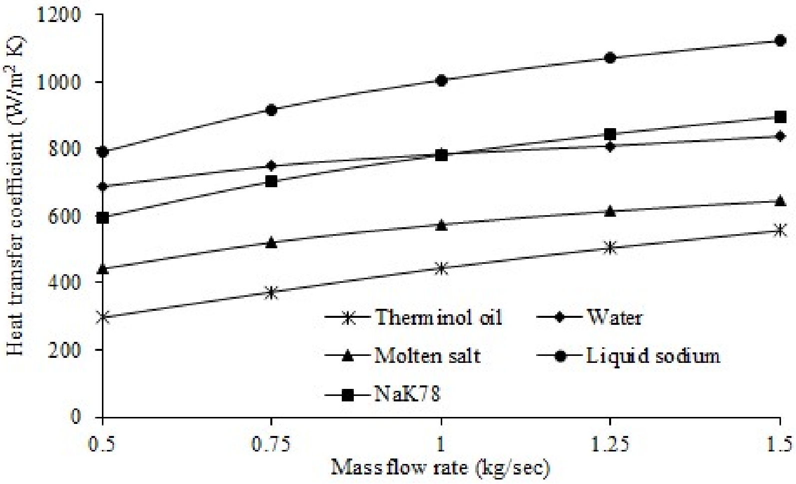

Fig. 5: Heat transfer coefficient for the absorber of PTC with non-uniform heat flux boundary condition

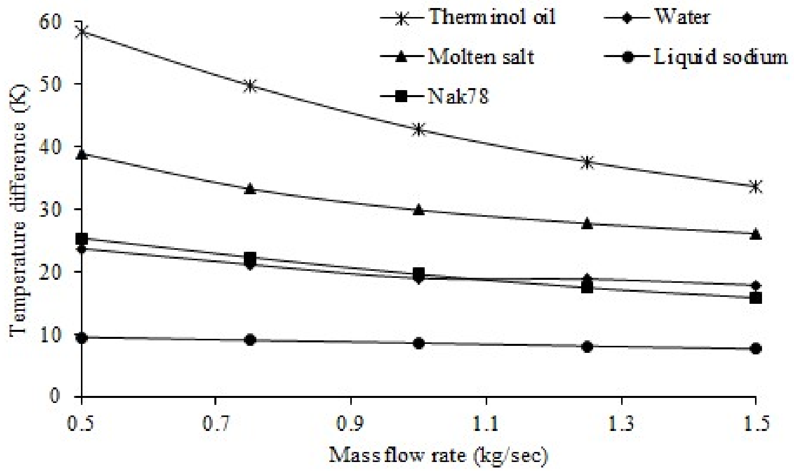

Fig. 6: Temperature difference between absorber wall and mean fluid temperature for various HTF's with non-uniform heat flux boundary condition

The temperature difference around the circumference of the absorber wall is maximum for lower mass flow rate and decreases with increase in mass flow rate. The temperature difference around the circumference is maximum for therminol oil at 0.5 kg/s of mass flow rate and minimum for liquid sodium at 1.5 kg/s. Higher the temperature difference results in thermal stress in the absorber wall. It leads to deflection of the absorber, results in poor optical efficiency. Hence, it is clear that thermo-physical properties of HTF's play an important role in performance of the receiver.

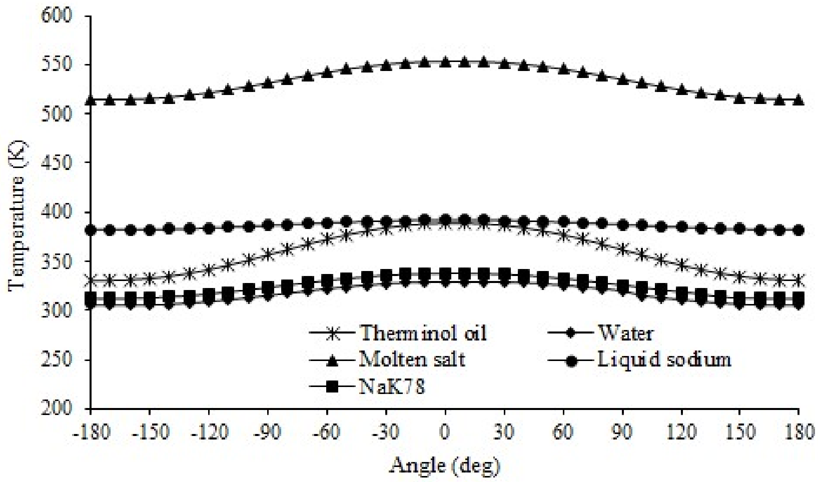

Fig. 7: Temperature of the absorber tube around the circumference for mass flow rate of 0.5 kg/s

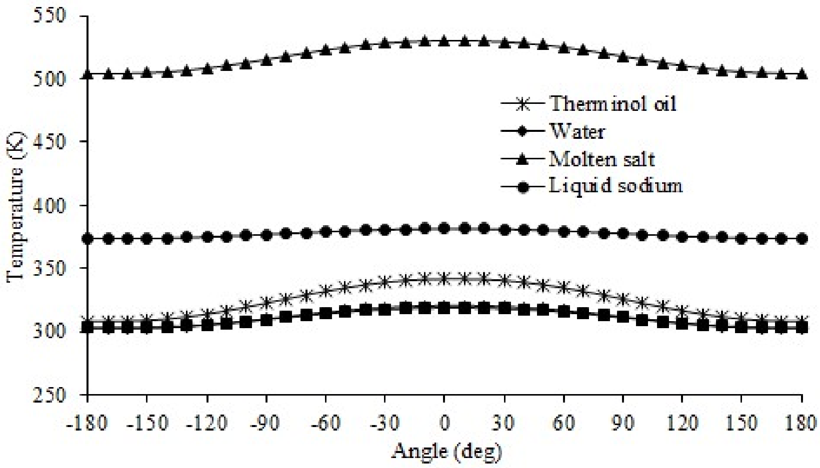

Fig. 8: Temperature of the absorber tube around the circumference for mass flow rate of 1.5 kg/s

Tab. 2: Temperature difference around the absorber circumference for different working fluids

Heat Transfer Fluids	**Temperature (K)**				
Mass flow rate (kg/s)	**0.5**	**0.75**	**1**	**1.25**	**1.5**
Therminol oil	58.45	49.79	42.74	37.56	33.59
Water	23.67	21.12	18.94	18.8	17.79
Molten salt	38.89	33.22	29.84	27.68	26.09
Liquid sodium	9.49	9.01	8.58	8.09	7.65
Nak78	25.37	22.27	19.55	17.4	15.8

The temperature contours along the length for therminol oil, water and Nak78 are sown in Fig.9 at 0.5 kg/s. The temperature increases gradually along the length from inlet temperature of 300 K. Temperature contours of molten salt and liquid sodium is shown in Figure 10 and 11 respectively.

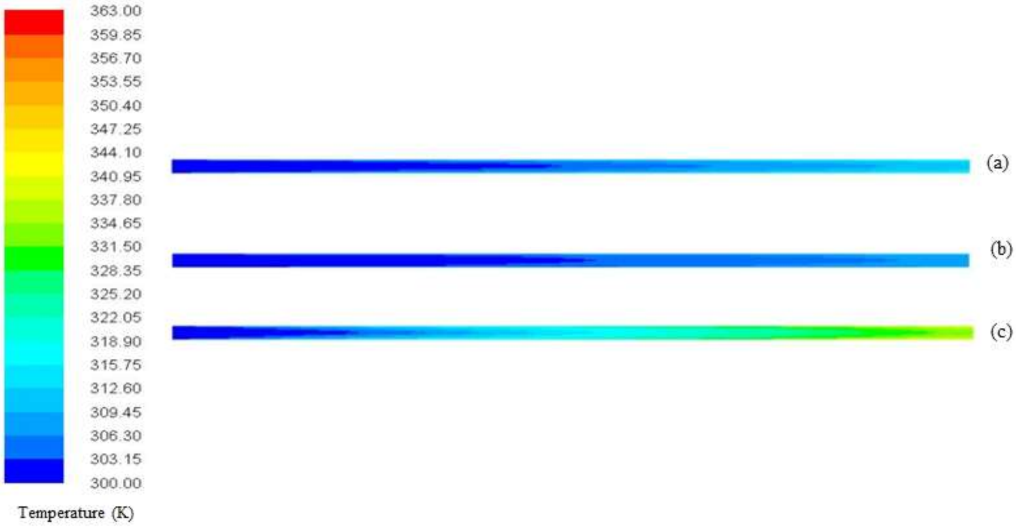

Fig. 9: Temperature contours for (a) Therminol, (b) Water, (c) NaK78 at 0.5 kg/sec mass flow rate with non-uniform heat flux

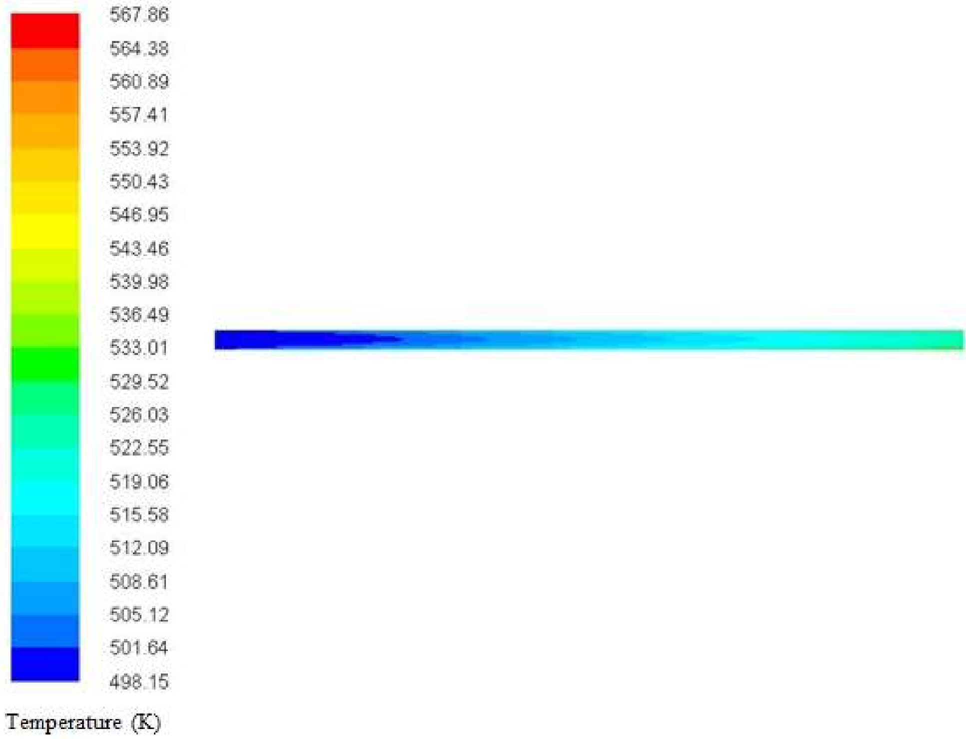

Fig. 10: Temperature contours for molten salt at 0.5 kg/sec mass flow rate with non-uniform heat flux

The temperature contours at the outlet of the absorber tube for therminol oil, water and NaK78 are shown in Figure 12. NaK78 achieves higher outlet temperature due to low specific heat and higher thermal conductivity. The temperature at outlet of absorber tube for various HTF's such as therminol oil, water and NaK78 at 0.5 kg/s are found as 314.3 K, 308.57 K and 337.3 K respectively. Figure 13 and 14 shows the temperature contours at the outlet of absorber for molten salt and liquid sodium respectively. The outlet temperature of the molten salt and liquid sodium is calculated as 527.6 K and 398.8 K respectively for 0.5 kg/s.

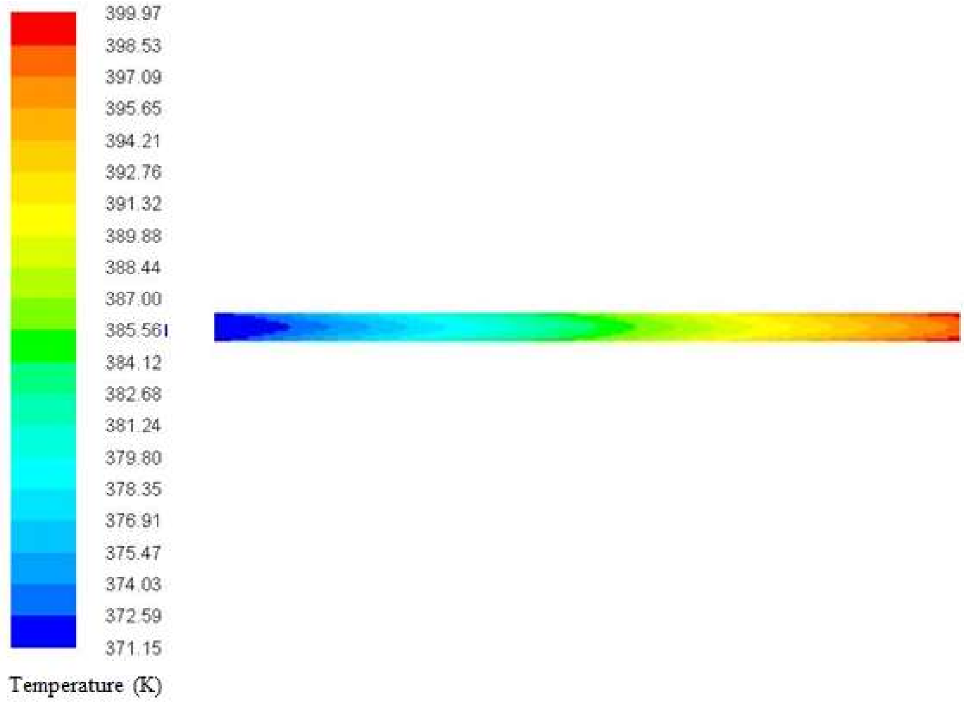

Fig. 11: Temperature contours for liquid sodium at 0.5 kg/sec mass flow rate with non-uniform heat flux

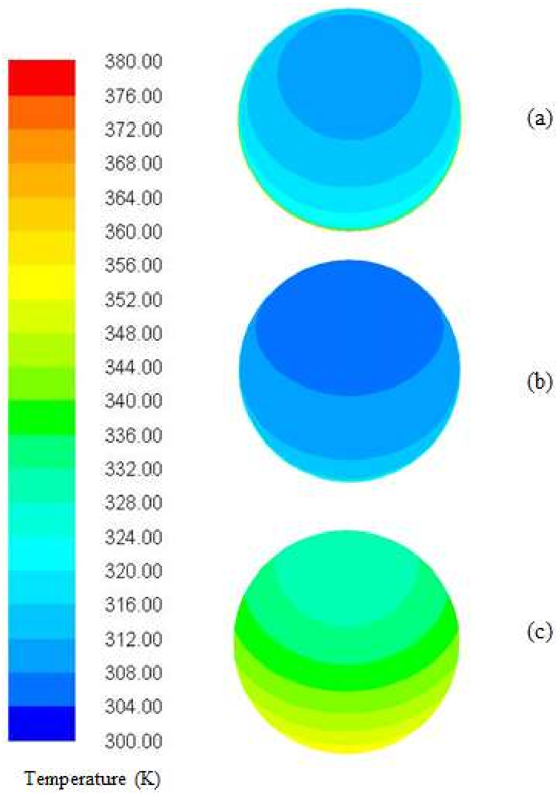

Fig. 12: Temperature contours at outlet of the absorber for (a) Therminol oil (b) water and (c) NaK78 at 0.5 kg/s with non-uniform heat flux distribution

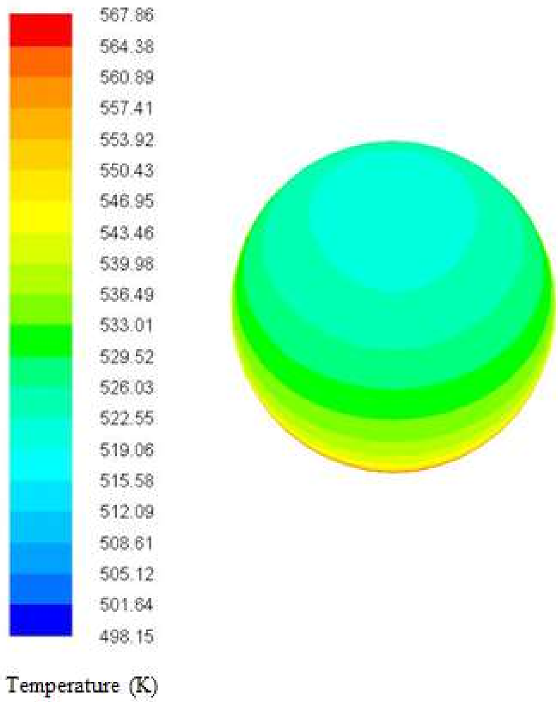

Fig. 13: Temperature contour at outlet of the absorber for molten salt at mass flow rate of 0.5 kg/s

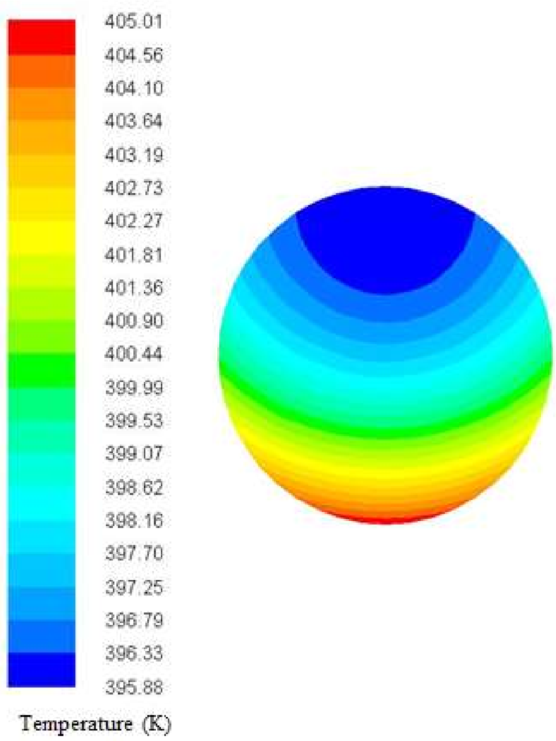

Fig.14: Temperature contour at outlet of the absorber for liquid sodium at mass flow rate of 0.5 kg/s

Based on the analysis, it is found that liquid sodium and NaK78 offers less temperature difference around the circumference of the absorber as well as temperature difference between the inner wall of the absorber to the mean temperature of the fluid as compared to other heat transfer fluids. Since melting temperature of the liquid sodium (97.82^{o}C) is higher than the ambient, it requires either option for draining of liquid sodium from the receiver or trace heating during plant startup. It increases plant operating cost which is not desirable. The melting point of NaK78 is12.6^{o}C which is less than the ambient temperature for most of the climatic conditions. It is desirable to use Nak78 as heat transfer fluid for parabolic trough solar collector to improve the performance of the absorber significantly.

7. Conclusions

The numerical simulation of absorber for a parabolic trough solar collector has been carried out for different HTF's and observed that the liquid sodium and NaK78 performs better than other HTF's due to its high thermal conductivity. It also reduces the temperature gradient between the absorber wall surface to the mean fluid temperature as well as around the absorber circumference. Hence it helps to reduce the heat losses from the absorber of the parabolic trough solar collector. By reducing the circumferential temperature difference, thermal stress in the absorber tube can be minimized which results in no / minimum deflection of the absorber in turn it improves the intercept factor / optical efficiency of the parabolic trough solar collector. Overall, using liquid metal as heat transfer fluid improves the overall performance of the parabolic trough solar collector. Since liquid sodium and NaK78 violently reacts with water and air, special precautions should be taken care to avoid the safety related issues.

8. References

Almanza, R., Lentz, A., Jimenez, G., 1997. Receiver behavior in direct steam generation with parabolic troughs. Sol Energy, 61(4), 275-278.

Boerema, N., Morrison, G., Taylor, R., Rosengarten, G., 2012. Liquid sodium versus Hitec as a heat transfer fluid in solar thermal central receiver systems. Solar Energy, 86, 2293–2305.

Cheng, Z. D., He, Y. L., Xiao, J., Tao, Y. B., Xu, R. J., 2010. Three-dimensional numerical study of heat transfer characteristics in the receiver tube of parabolic through solar collector. Int. Communications in Heat and Mass Transfer, 37, 782-787.

FLUENT, 2016. ANSYS Fluent theory guide, ANSYS, Inc. Canonsburg, PA 15317.

Khanna, S., Sharma, V., 2016. Explicit analytical expression for solar flux distribution on an undeflected absorber tube of parabolic trough concentrator considering sun-shape and optical errors, J. of Solar Energy Engineering, 138, 1-10.

Kotze, J. P., Backstrom, T. W. V., Erens, P. J., 2012. NaK as a primary heat transfer fluid in thermal solar power installations, 1st Southern African Solar Energy Conference (SASEC), 1-9.

Kumar, K. R., Reddy, K. S., 2009. Thermal analysis of solar parabolic trough with porous disc receiver, Applied energy, 86, 1804-1812.

Kumar, K. R., Reddy, K. S., 2012. Effect of porous disc receiver configurations on performance of solar parabolic trough concentrator, Heat Mass Transfer, 48, 555-571.

NREL (National Renewable Energy Laboratory), (2017). Accessed on 6th January 2017, from Concentrating Solar Power Projects by Project Name: https://www.nrel.gov/csp/solarpaces/by_project.cfm

Odeh, S. D., Morrison, G. L., Behnia, M., 1998. Modelling of parabolic trough direct steam generation solar collectors, Solar Energy, 395-406.

Pacio, J., Fritsch, A., Singer, C., Uhlig, R., 2014. Liquid metals as efficient coolants for high-intensity point-focus receivers: implications to the design and performance of next generation CSP systems, Energy Procedia, 49; 647-655.

Srivastva, U., Malhotra, R. K., Kaushik, S. C., 2015. Recent developments in heat transfer fluids used for solar thermal energy applications, Fundam. Renewable Energy Appl., 5(6), 1-11.

9. Nomenclature

C_p	Specific heat (J/kg K)
d_i	Inner diameter (m)
d_o	Outer diameter (m)
h_f	Heat transfer coefficient (W/m^2 K)
k	Turbulent kinetic energy (m^2/s^2)
L	Length of cylinder (m)
Pr	Prandtl number
q	Heat flux (W/m^2)
r	Radius (m)
Re	Reynolds number
T	Temperature (K)
T_{in}	Inlet temperature (K)
T_{ref}	Reference temperature (K)
T_w	Wall temperature (K)
u_{in}	Inlet velocity (m/s)
u_i, u_j	Velocity (m/s)
θ	Angle (deg)
ρ	Density (kg/m^3)
μ	Dynamic viscosity (N s/m^2)
ε	Turbulent dissipation rate (m^2/s^3)